# TREM2 blockade reprograms HER2 CAR macrophages toward inflammatory phagocytes in breast cancer models

**Marius Jassaud**
Univ. Lille, Inserm, CHU Lille, U1192 - Protéomique Réponse Inflammatoire Spectrométrie de Masse - PRISM

**Lydia Ziane-Chaouche**
Univ. Lille, Inserm, CHU Lille, U1192 - Protéomique Réponse Inflammatoire Spectrométrie de Masse - PRISM

**Antonella Raffo-Romero**
Univ. Lille, Inserm, CHU Lille, U1192 - Protéomique Réponse Inflammatoire Spectrométrie de Masse - PRISM

**Michel Salzet**
Univ. Lille, Inserm, CHU Lille, U1192 - Protéomique Réponse Inflammatoire Spectrométrie de Masse - PRISM

**Marie Duhamel**
marie.duhamel@univ-lille.fr

Univ. Lille, Inserm, CHU Lille, U1192 - Protéomique Réponse Inflammatoire Spectrométrie de Masse - PRISM

---

**Research Article**

**Keywords:** TREM2, CAR macrophages, breast cancer, phagocytosis, immunotherapy, tumor-associated macrophages

**Posted Date:** June 5th, 2026

**DOI:** https://doi.org/10.21203/rs.3.rs-9679135/v1



**Additional Declarations:** No competing interests reported.

# Abstract

Tumor-associated macrophages (TAMs) are key regulators of the breast tumor microenvironment and often display immunosuppressive functions that limit cellular immunotherapy efficacy. Triggering receptor expressed on myeloid cells 2 (TREM2) has emerged as a critical modulator of myeloid cell activity and a potential target to enhance the anti-tumor activity of engineered macrophages. Here, we show that TREM2 is enriched in breast cancer transcriptomic datasets and correlates with myeloid and immunoregulatory gene networks. Using HER2-directed CAR macrophages (CAR-M) generated from THP-1 cells, we found that anti-inflammatory stimulation increased TREM2 expression. Genetic or pharmacological inhibition of TREM2 reduced CAR-M anti-inflammatory polarization. Data-independent acquisition proteomics showed that TREM2 blockade attenuated IL-4/IL-13/IL-10-associated programs while enhancing inflammatory, interferon-related, cytoskeletal and metabolic signatures. Functionally, TREM2 inhibition enhanced HER2-dependent phagocytosis in both cell lines and patient-derived tumoroid models. These findings identify TREM2 as a macrophage-intrinsic immune checkpoint limiting CAR-M activity and support its targeting to improve macrophage-based immunotherapies in breast cancer.


# Introduction

Macrophages are highly plastic innate immune cells that play central roles in immune homeostasis and host defense. In cancer, macrophages represent a major population within the tumor microenvironment (TME), where they are commonly referred to as tumor-associated macrophages (TAMs)[1]. Rather than exerting antitumor functions, TAMs are often reprogrammed by tumor-derived signals toward immunosuppressive, tumor-promoting states. Although TAM phenotypes are heterogeneous, M2-like populations frequently predominate in established tumors, promoting immune suppression, angiogenesis, invasion and metastasis[2]. High TAM density is consistently associated with poor clinical outcomes across multiple cancer types[3].

Given their abundance in tumors and intrinsic effector functions, macrophages are attractive targets for therapeutic reprogramming. Chimeric antigen receptor–engineered macrophages (CAR-M) redirect macrophages toward tumor cells and enhance antitumor functions through antigen-specific phagocytosis and cytokine production[4]. In solid tumors, where CAR-T therapies often fail, CAR-M represent a promising strategy, although their efficacy remains constrained by immunosuppressive signals that limit macrophage activation. Several engineering strategies have been developed to reinforce pro-inflammatory CAR-M programs[5],[6],[7, 8].

Although these strategies enhance CAR-M activation, effective tumor clearance ultimately depends on phagocytosis. Tumor cells evade macrophage-mediated clearance through the upregulation of antiphagocytic “don’t eat me” signals, which engage inhibitory receptors and restrain engulfment[9, 10]. Targeting these phagocytic checkpoints enhances macrophage phagocytosis, modulates TAM polarization, and reshapes cytokine secretion. Among these, triggering receptor expressed on myeloid

cells 2 (TREM2) has emerged as a central regulator of immune suppression in cancer. TREM2, a transmembrane receptor signaling via the adaptor protein DNAX-activating protein of 12 kDa (DAP12), was initially studied in Alzheimer's disease[11, 12] but is now recognized as a key macrophage-intrinsic checkpoint in tumors. It binds diverse ligands, including lipoproteins and anionic lipids, though their relevance in the TME remains unclear. TREM2 is broadly expressed by TAMs[13] and defines a population with potent immunosuppressive activity[14, 15]; disruption of TREM2 signaling promotes pro-inflammatory polarization and enhances tumor cell phagocytosis[16]. The abundance of $TREM2^+$ TAMs correlates with tumor progression and poor patient outcomes across multiple cancers.

Building on these observations, we evaluated the impact of TREM2 inhibition on CAR-M function using both genetic and pharmacological approaches. Macrophage phenotypes were assessed through comprehensive mass spectrometry–based proteomics and targeted qPCR, and tumor cell–phagocytic capacity was measured. This integrated strategy allowed us to examine how relieving TREM2-mediated suppression modulates CAR-M polarization and enhances their antitumor activity.

## Materials and Methods

# Cell Culture

THP-1 and AU565 cell lines were maintained in RPMI 1640 medium supplemented with 10% fetal bovine serum (FBS), 2 mM L-glutamine, and 100 U/mL penicillin/streptomycin. MDA-MB-231 cells were cultured in DMEM supplemented with 10% FBS, 2 mM L-glutamine, and 100 U/mL penicillin/streptomycin. All cell lines were maintained at 37°C in a humidified incubator with 5% CO2.

Breast cancer–derived tumoroids were generated from patient tumor tissues. The study was approved by the local research committee of the Oscar Lambret Cancer Center and a French Ethical Committee (IdRCB 2021-A00670-41). The HCI-032 tumoroid line was kindly provided by Dr. Alana Welm (Huntsman Cancer Institute, University of Utah)[17]. Written informed consent for the study was obtained from the patients. Tumoroids were cultured as previously described[18]. Primary macrophages derived from human PBMCs were purified as previously described[18].

## Plasmid construction and viral vectors

The HER2-specific CAR construct consisted of a CD8α signal peptide, trastuzumab-derived scFv, a hinge region, a CD8α transmembrane domain, and a CD3ζ intracellular signaling domain. The sequence was cloned into a lentiviral vector under the control of the EF1α promoter, with EGFP expression driven by a CMV promoter. A mock vector lacking the CAR sequence was used as a control.

For TREM2 silencing, a plasmid encoding a short hairpin RNA (shRNA) targeting human TREM2 was generated under a U6 promoter, along with a puromycin resistance cassette for selection. A non-targeting scrambled shRNA was used as a control. Target sequences are listed in **Supp.Table 1.**

All plasmid construction and lentiviral production were performed by VectorBuilder.

## Viral transduction

THP-1 monocytes were transduced with lentiviral particles at a multiplicity of infection (MOI) of 10 in the presence of polybrene (8 µg/mL), followed by centrifugation at 1,000 × g for 60 min to enhance viral entry. Cells were then cultured in fresh complete culture medium.

CAR-expressing cells were sorted based on GFP expression, using an SH800 cell sorter (Sony, Inc.). TREM2 knockdown cells were selected using puromycin (2 µg/mL). Following knockdown, cells were re-sorted to obtain homogenous CAR expression between shScramble and shTREM2 conditions.

Macrophage differentiation was induced using phorbol 12-myristate 13-acetate (PMA, 100 ng/mL) in complete medium for 24, 48 or 72h. Cells were either harvested immediately or left to rest for 24 h in fresh medium. Based on these experiments, a differentiation period of 72 h followed by a 24 h resting phase was used for all subsequent experiments.

Differentiated macrophages were treated with IFN-γ (20 ng/mL) or IL-4/IL-10 (20 ng/mL each) or left untreated, for 24 h prior to downstream analysis.

## Pharmacological inhibition of TREM2

Pharmacological inhibition was achieved using the small-molecule inhibitor TREM2-in-1 (iTREM2, MedChemExpress). After differentiation, THP-1-derived macrophages were treated with iTREM2 for 24 h. Dose-response experiments (1, 5, and 10 µM) were performed to assess TREM2 inhibition by Western blot. For subsequent experiments, cells were treated with 10 µM iTREM2 for 24h. Where indicated, macrophages were stimulated with IFN-γ (20 ng/mL) or IL-4/IL-10 (20 ng/mL each) in the presence or absence of the inhibitor. Control cells were treated with DMSO.

## Viability tests

Cells were plated in 96-well plates and treated with iTREM2 (10 µM) for 24 or 48 h. Cell viability was assessed using an MTS assay (CellTiter 96® AQueous One Solution, Promega), according to the manufacturer's instructions. Absorbance was measured at 490 nm, and values were proportional to the number of metabolically active cells.

# RT-qPCR

Total RNA was extracted using TRIzol reagent (QIAGEN) according to the manufacturer's instructions. cDNA was synthesized from 1 µg of RNA using SuperScript® III Reverse Transcriptase (Invitrogen). Quantitative real-time PCR was performed using SYBR™ Green Master Mix (Applied Biosystems). A no-

reverse transcription control (–RT) was included to assess genomic DNA contamination. Primer sequences are listed in **Supp.Table 1**.

## Protein extraction and Western Blot analysis

Cells were lysed in RIPA buffer supplemented with protease inhibitors. Protein concentrations were determined using the Bradford assay. Equal amounts of protein (30µg) were separated by SDS-PAGE and transferred onto nitrocellulose membranes. Membranes were blocked and incubated with primary antibodies (anti-TREM2, 1/1000, Abcam) overnight at 4°C, followed by HRP-conjugated secondary antibodies (anti-rabbit HRP, 1/15000, Abcam) for 1 h at room temperature. Protein bands were detected by chemiluminescence (West Dura, Pierce) and imaged using the iBright™ CL750 Imaging System (Invitrogen).

## Flow cytometry

CAR, TREM2, and CD11b expression in THP1-derived macrophages were assessed by flow cytometry. For CAR detection, cells were incubated with a biotinylated HER2 recombinant protein (ACROBiosystems), followed by staining with a PE-conjugated anti-biotin antibody (1:100, Miltenyi Biotec). Cells were then washed, fixed with 4% PFA, and resuspended in PBS containing 1% FBS. CAR expression was determined as the percentage of PE-positive cells. TREM2 and CD11b expression were analyzed using specific antibodies (R&D System and BD Biosciences, respectively).

For HER2 expression analysis in patient-derived tumoroids, samples were dissociated using TrypLE, washed and stained with a PE-conjugated anti-human HER2 antibody (BD Biosciences), followed by fixation.

All samples were analyzed using a CytoFLEX LX cytometer (Beckman Coulter). Isotype controls were included and data were processed using KALUZA software.

# Phagocytosis assay

# Flow cytometry-based assay

THP-1-derived CAR-M, either treated with iTREM2 (10µM), or expressing shScramble/shTREM2, were stimulated or not with IFN-γ (20ng/ml) for 24 h and co-cultured with AU565 (HER2+) or MDA-MB-231 (HER2-) tumor cells. Co-cultures were performed at a 3:1 effector-to-target ratio for 6 or 24 h at 37°C. Tumor cells were pre-labeled with Cytotell™ Blue (AAT Bioquest) prior to co-culture. Following co-culture, cells were collected and analyzed by flow cytometry (CytoFLEX LX, Beckman Coulter). Phagocytosis was quantified as the percentage of double-positive ($Cytotell^{+}GFP^{+}$) cells.

For 3D assays, shScramble or shTREM2 CAR-HER2 macrophages were co-cultured with $HER2^+$ tumoroids in non-adherent plates in tumoroid medium supplemented with 2% Matrigel, at a 3:1 ratio for 48 h, as previously described[6]. Phagocytosis was assessed by flow cytometry as described above.

# Microscopy-based assay

For imaging, THP-1 CAR-M were seeded on poly-D-lysine–coated coverslips and co-cultured with Cytotell™ Blue-labeled AU565 cells at a 3:1 ratio for 6 h. Cells were fixed with 4% PFA, stained with SYTOX™ Deep Red, and imaged using a Zeiss LSM 510 confocal microscope. Image analysis was performed using ImageJ.

# Proteomic sample preparation

THP-1 monocytes expressing mock or CAR-HER2 constructs, either with shScramble/shTREM2 or treated with iTREM2 (10μM), were differentiated as described above and subsequently left untreated or stimulated for 24 h with IFN-γ (20 ng/mL), or IL-4/IL-10 (20 ng/mL each). Cells were then lysed in RIPA buffer, and protein concentrations were determined using the Bradford assay.

For proteomic analysis, 50 μg of total protein per condition were processed using the filter-aided sample preparation (FASP) protocol. Briefly, proteins were reduced, alkylated and digested overnight with sequencing-grade trypsin (Promega, 40 μg/mL). Peptide digestion was quenched by addition of trifluoroacetic acid (TFA, 0.5%).

Peptides were prepared for liquid chromatography–tandem mass spectrometry (LC–MS/MS) analysis using the Evotip Pure system (Evosep) according to the manufacturer's instructions.

# LC-MS/MS analysis

Peptides were analyzed on an Evosep One system coupled with a timsTOF HT mass spectrometer (Bruker Daltonics).The Evosep One was operated with the 60 Samples Per Day method, using a C18 reverse-phase column (EV1109; 8 cm × 150 μm, 1.5 μm particle size), maintained at 40°C. The column outlet was interfaced with a fused silica emitter (10 μm inner diameter, Bruker Daltonics), connected to a CaptiveSpray ion source (Bruker). Data acquisition was performed in DIA-PASEF mode over an m/z range of 100–1700 and an ion mobility separation window from 1/K0 = 1.51 V cm − 2 to 1/K0 = 0.6 V cm − 2.

# Raw data analysis

Raw MS data were processed using DIA-NN software (v2.1.0)[19, 20] using a library-free approach against the UniProtKB human database (May 2023, 20,420 entries), with trypsin specificity, up to two missed cleavages, methionine oxidation as variable modification, and cysteine carbamidomethylation as fixed modification. Peptides were considered within a length range of 7 to 30 amino acids, with precursor charges between + 2 and + 4. Precursor and fragment ion m/z ranges were set to 100–1700 and 300–1300, respectively. Peptide and protein identifications were controlled at 1% FDR. The "match between runs" feature was activated.

Downstream statistical analyses were performed using Profiler software (v 1.2)[21]. Proteins consistently detected across samples were retained for analysis. Data cleaning was performed within the DataLab module. Data preprocessing included applying a minimum feature detection threshold of 66% per class. Missing values were imputed on a per-class basis using a shifted Gaussian distribution method (downshift = 1.8 standard deviations; width = 0.3 standard deviations), as commonly applied in proteomics analyses. Features that remained entirely missing in at least one class after imputation were excluded from further analysis. Heatmaps were generated using the Biomarker module, considering all detected features; however, only proteins with significant differential expression (p-value < 0.01) were retained for visualization. For box plot representation of protein expression levels, LFQ intensity values were log2-transformed. Statistical analyses were performed using GraphPad Prism, using Student's t-test or one-way ANOVA as appropriate.

# Pathway analysis

Differentially expressed proteins were subjected to pathway enrichment analysis using the Reactome database (V96). Enrichment was assessed using a hypergeometric test with Benjamini-Hochberg correction. Visualizations were generated in R using the ggplot2 package as bubble plots.

# Gene expression analysis in breast cancer datasets

Gene expression analysis was performed using publicly available RNA-seq data from the TCGA Breast Invasive Carcinoma cohort. TREM2 expression in tumor and normal tissues was analyzed using the GEPIA2 web server, and expression across molecular subtypes was assessed using cBioPortal. Correlation between TREM2 and immune-related genes was evaluated using Spearman correlation analysis. Dot plot visualization was performed in R using the ggplot2 package.

# Experimental Design and Statistical Rationale

For MS-based proteomics, each condition was analyzed using three independent biological replicates derived from separate cell cultures, protein extractions, and enzymatic digestions. Acquisition order was randomized to minimize batch effects. For all other assays, experiments were performed in at least three independent biological replicates and data are presented as mean ± standard error. Statistical analyses were conducted using GraphPad Prism, with differences assessed using Student's t-test or one-way ANOVA. Statistical significance was defined as ****P < 0.0001, ***P < 0.001, **P < 0.01, *P < 0.05.

## Results

**TREM2 is upregulated in breast cancer and associated with immune-related transcriptional programs.**

To investigate the clinical relevance of TREM2 in breast cancer, we analyzed its expression in tumor versus normal tissues using TCGA publicly available transcriptomic data. TREM2 expression was significantly increased in breast cancer samples compared to normal tissue, indicating a tumor-associated enrichment (**Fig. 1a**).

TREM2 expression also varied across molecular subtypes, with higher observed in Luminal and HER2-positive tumours compared to the basal-like subtype (**Fig. 1b**).

Correlation analysis further revealed that TREM2 expression was strongly associated with myeloid and immunoregulatory gene signatures, including genes related to macrophage identity and TREM2 signalling (TYROBP, SPI1, AIF1, LAPTM5, LRRC25, MSR1), immunosuppressive and checkpoint-like pathways (HAVCR2, SIGLEC9, CD33, CD300A/C, TNFAIP8L2), and complement and phagocytic immune functions (C1QA, C1QB, C1QC, FCGR family members, C3AR1, ITGAX, DPEP2). (**Fig. 1c**). These findings indicate that TREM2 is embedded within a tumor-associated macrophage transcriptional network combining immune activation and immunosuppressive features.

Together, these results demonstrate that TREM2 is enriched in breast cancer, and associated with macrophage-related immunoregulatory programs, supporting a potential role in shaping the tumor immune microenvironment.

**Figure 1 TREM2 is upregulated in breast cancer and associated with a myeloid immune transcriptional program.**

1. (a) TREM2 expression in breast cancer (BRCA) compared to normal breast tissue using TCGA RNA-seq data, showing increased expression in tumor samples.
2. (b) TREM2 mRNA expression across breast cancer molecular subtypes (Basal-like, HER2-enriched, Luminal A, and Luminal B) using TCGA data, represented as z-scores relative to normal tissues.
3. (c) Spearman correlation analysis of TREM2 expression with immune-related genes in breast cancer samples. Dot size represents statistical significance (-log10 p-value) and color intensity represents correlation strength ($R^2$).

# Anti-inflammatory polarization induces TREM2 expression in optimized CAR-M

Since TREM2 was enriched in breast cancer and associated with macrophage-related immunoregulatory programs, we generated HER2-targeting CAR-M to investigate its role in a therapeutic context, using THP-1 cells as a widely used model for macrophage differentiation.

We next optimized THP1 differentiation to generate macrophage-like CAR-M while maintaining stable CAR expression. THP1-CAR monocytes were differentiated using PMA for 24, 48, or 72 h, followed by an optional 24 h resting period in PMA-free medium (**Fig. 2a**). Macrophage differentiation and CAR expression were assessed by flow cytometry through CD11b expression and CAR levels, measured as percentage of positive cells and mean fluorescence intensity (MFI).

Increasing PMA exposure promoted macrophage differentiation, as shown by increased CD11b expression, with maximal levels observed after 72 h of PMA treatment followed by a 24 h resting period (**Fig. 2b-d**). CAR expression remained high across conditions (> 90% positive cells) (**Fig. 2e-f**), but its

expression levels (MFI) increased with differentiation, reaching a maximum under the 72 h + resting condition (**Fig. 2g**).

Based on these results, 72 h of PMA differentiation followed by a 24 h resting period was selected for subsequent experiments.

We next assessed whether macrophage polarization regulates TREM2 expression. Mock macrophages and CAR-M were stimulated under pro-inflammatory (IFN-γ) or anti-inflammatory (IL-4/IL-10) conditions. Anti-inflammatory polarization significantly increased TREM2 expression in both cell types, whereas IFN-γ had limited effects (**Fig. 2h-i**). Consistently, anti-inflammatory stimulation increased TREM2 expression in primary human monocyte-derived macrophages at both the protein and mRNA levels (**Supp. Figure 1a-b**).

These results indicate that anti-inflammatory signals promote TREM2 expression in CAR-M.

**Figure 2 Optimization of HER2 CAR macrophage differentiation and regulation of TREM2 expression by macrophage polarization**

1. (a) Experimental design illustrating the differentiation and resting kinetics of CAR-HER2 kinetics of CAR-HER2 monocytes at 24 h, 48 h, and 72 h.
2. (b) Representative flow cytometry histograms showing CD11b expression in CAR-HER2 monocytes at different time points, with or without a resting phase.

(c-d) Quantification of CD11b expression, shown as the percentage of $CD11b^+$ cells and mean fluorescence intensity (MFI) (n = 3).

(e) Representative histograms of CAR expression in CAR-HER2 cells with or without a resting phase.

(f-g) Quantification of CAR expression, shown as the percentage of CAR-positive cells and MFI (n = 3).

(h-i) TREM2 expression (MFI) at 24 h and 48 h following stimulation with IFNγ or IL-4/IL-10 (n = 3).

# TREM2 inhibition modulates macrophage polarization in CAR-M

Given that anti-inflammatory polarization induced TREM2 expression in CAR-M, we next investigated whether TREM2 inhibition could modulate CAR-M phenotype. TREM2 was inhibited using both genetic and pharmacological approaches, and macrophage polarization was assessed by qPCR analysis of macrophage-associated genes.

For genetic inhibition, TREM2 expression was silenced using shRNA in both mock macrophages and HER2 CAR-M. Efficient knockdown was confirmed at the mRNA level by qPCR and at the protein level by Western blot (**Fig. 3a-c**), showing a marked reduction in TREM2 expression in shTREM2 cells compared

to controls (scramble shRNA, Scr). Following shRNA transduction, CAR-M were re-sorted by flow cytometry to ensure a homogeneous CAR-positive population. CAR expression was subsequently confirmed by flow cytometry, demonstrating comparable expression levels between scramble and shTREM2 CAR-M (**Supp. Figure 2a-b**).

We next evaluated the impact of TREM2 inhibition on macrophage polarization (**Fig. 3d).** Cells were stimulated under pro-inflammatory (IFN-γ) or anti-inflammatory (IL-4/IL-10) conditions, and compared to basal conditions. TREM2 silencing reduced the expression of anti-inflammatory markers, including IL-10 and CD206, under IL-4/IL-10-stimulation (**Fig. 3d**). In contrast, pro-inflammatory genes such as TNF-α and CXCL9 were similarly induced by IFN-γ in both control and shTREM2 cells (**Fig. 3d**).

**Figure 3 Genetic inhibition of TREM2 modulates macrophage polarization in HER2 CAR macrophages**

1. (a) Relative TREM2 mRNA expression in mock and CAR-HER2 macrophages transduced with scramble or shTREM2 constructs (n = 3).
2. (b) Representative Western blot analysis of TREM2 protein expression in mock and CAR-HER2 macrophages, with β-actin as a loading control (n = 3).
3. (c) Quantification of TREM2 protein expression relative to β-actin (n = 3).
4. (d) Relative mRNA expression of polarization-associated genes in CAR-HER2 macrophages (scramble vs shTREM2) under basal conditions or following stimulation with IFNγ or IL-4/IL-10 (n = 3).

To confirm these findings, we performed pharmacological inhibition of TREM2 in CAR-M. The inhibitor used in this study is derived from oxaliplatin and artesunate and has been previously reported to inhibit TREM2 in macrophages[22]. Treatment with the TREM2 inhibitor resulted in a dose-dependent reduction of TREM2 protein levels, with a marked decrease at 10 μM (**Fig. 4a-b**). This concentration was therefore selected for subsequent experiments.

Consistent with genetic silencing, pharmacological inhibition reduced the expression of anti-inflammatory markers (IL-10, CD206) and slightly increased TNF-α under basal conditions, while attenuating IL-4/IL-10-induced responses. No major differences were observed under IFN-γ stimulation (**Fig. 4c**).

Together, these results show that TREM2 inhibition limits anti-inflammatory polarization in CAR-M.

**Figure 4 Pharmacological inhibition of TREM2 modulates macrophage polarization in HER2 CAR macrophages.**

1. (a) Western blot analysis of TREM2 protein expression following treatment with increasing concentrations of the TREM2 inhibitor (iTREM2), with β-actin as a loading control (n = 3).
2. (b) Quantification of TREM2 protein expression following iTREM2 treatment. TREM2 levels were normalized to β-actin and expressed as fold change relative to untreated control macrophages (n = 3).

3. (c) Relative mRNA expression of polarization-associated genes (TNF-α, CXCL9, IL-10 and CD206) in CAR-HER2 macrophages under basal conditions or following stimulation with IFN-γ or IL-4/IL-10, in the presence or absence of the TREM2 inhibitor (iTREM2) (n = 3).

# TREM2 inhibition reshapes the proteomic landscape of CAR-M

To further characterize the molecular mechanisms underlying TREM2-mediated regulation of macrophage function, we performed global proteomic analysis of CAR-M following TREM2 knockdown. A total of 4,562 proteins were identified, of which 330 were differentially expressed between scramble and shTREM2 CAR-M (**Supp.Table 2).**

Unsupervised clustering revealed two distinct proteomic profiles separating control and TREM2-deficient CAR-M (**Fig. 5a**). Pathway enrichment analysis showed that control CAR-M were enriched in IL-4, IL-13, and IL-10 signaling pathways, consistent with an immunoregulatory, TAM-like phenotype (**Fig. 5b, Supp. Figure 3**). In contrast, TREM2-deficient CAR-M displayed enrichment in type I and II interferon signaling pathways, including IFNα/β and IFNγ responses, supported by increased expression of interferon-stimulated proteins such as STAT1, BST2, and ISG20 (**Fig. 5c**)[23–25].

TREM2 knockdown was also associated with reduced expression of angiogenesis-related proteins, and immunosuppressive regulators such as SIRPA and CD300A (**Fig. 5c**). CD300A also correlated with TREM2 in breast cancer datasets (**Fig. 1c**), supporting its association with TREM2-dependent immunosuppressive programs. TAM-associated markers, including SPP1, CD44, and MSR1, were also downregulated (**Fig. 5c**). Conversely, pro-inflammatory-associated proteins such as PLD4 were upregulated.

TREM2 inhibition also induced metabolic reprogramming, characterized by reduced lipid metabolism and PPARα signaling, consistent with reduced expression of fatty acid metabolism-associated proteins such as CD36 and ACSL1 (**Fig. 5c**). This shift is consistent with a transition away from fatty acid oxidation, and supports enhanced macrophage activation. Interestingly, TREM2-deficient CAR-M also exhibited increased signatures of oxidative phosphorylation and aerobic respiration, indicating a potential rewiring of cellular metabolism toward alternative energy sources.

Under cytokine stimulation, TREM2-deficient CAR-M maintained a distinct proteomic profile, indicating a dominant role of TREM2 signaling (**Fig. 5d and Supp.Table 3**).

Under IL-4/IL-10 conditions, control CAR-M displayed enrichment in immunosuppressive proteins, including CD300A, COL6A1 and HMOX1, which were attenuated in TREM2-deficient cells (**Fig. 5e**).

In addition, TREM2-deficient CAR-M displayed reduced expression of SIRPA, SPP1, and CD44 across conditions. Under IFNγ stimulation, we also observed increased expression of CD70, a member of the TNF family associated with macrophage activation[26] (**Fig. 5e**).

Together, these results demonstrate that TREM2 inhibition induces broad proteomic and metabolic reprogramming of CAR-M, promoting a pro-inflammatory phenotype and limiting their responsiveness to immunosuppressive signals.

**Figure 5 Genetic inhibition of TREM2 reshapes the proteomic landscape of HER2 CAR macrophages.**

1. (a) Heatmap representation of the proteomic profile of THP-1 CAR-M following transduction with shTREM2 or scramble shRNA.
2. (b) Bubble plot showing enriched Reactome pathways in THP-1 CAR-M shTREM2 compared to scramble controls.
3. (c) Box plot representation of protein expression levels in THP-1 CAR-M shTREM2 versus scramble controls.
4. (d) Heatmap representation of the proteomic profile of THP-1 CAR-M (shTREM2 vs scramble) following stimulation with IFN-γ or IL-4/IL-10 for 24 h.

(e) Box plot representation of protein expression levels in THP1 CAR-M (shTREM2 vs scramble) under IFN-γ or IL-4/IL-10 stimulation for 24 h.

To determine whether these effects were recapitulated pharmacologically, we performed global proteomic analysis of CAR-M treated with the TREM2 inhibitor. A total of 6,060 proteins were identified, including 336 differentially proteins (**Supplementary Table 4**). Clustering analysis again revealed distinct profiles between control and iTREM2-treated cells (**Fig. 6a**).

Pathway analysis showed increased metabolic and inflammatory signaling and decreased IL-4/IL-13 pathways following TREM2 inhibition (**Fig. 6b** and **Supp. Figure 3**). Consistently, proteins involved in inflammatory signaling and cytoskeletal dynamics (e.g., BCL10, MAP4K2, FYB1) were upregulated, supporting enhanced NF-κB/MAPK activation and phagocytic potential (**Fig. 6c)**. Conversely, negative regulators of inflammatory signaling, such as DUSP4 and SIRT6, were reduced. In addition, immunoregulatory proteins, such as EBI3 were decreased (**Fig. 6c**).

Pharmacological inhibition also promoted metabolic reprogramming, with increased expression of glycolytic enzymes such as LDH1 and PDK2, consistent with a pro-inflammatory macrophage phenotype (**Fig. 6c**).

Under polarization conditions, a total of 256 proteins were differentially expressed across conditions (**Fig. 6d and Supp.Table 5**). iTREM2-treated CAR-M showed reduced anti-inflammatory signatures (e.g., CD163, S100A9) under IL-4/IL-10 stimulation, while maintaining or enhancing IFNγ-induced pro-inflammatory markers, such as TLR2 (**Fig. 6e**). Consistently, flow cytometry analysis in primary human macrophages showed that iTREM2 reduced anti-inflammatory marker expression (CD206, CD163) under IL-4/IL-10 stimulation (**Supp. Figure 4a-b).**

Together, these results demonstrate that pharmacological inhibition of TREM2 recapitulates the effects observed with genetic silencing, promoting a pro-inflammatory and anti-tumoral phenotype in CAR-M.

**Figure 6 Pharmacological inhibition of TREM2 reshapes the proteomic landscape of HER2 CAR macrophages.**

1. (a) Heatmap representation of the proteomic profile of THP-1 CAR-M following treatment with the iTREM2 inhibitor or control.
2. (b) Bubble plot showing enriched Reactome pathways in THP-1 CAR-M treated with iTREM2 compared to control.
3. (c) Box plot representation of protein expression levels in THP-1 CAR-M treated with iTREM2 versus control.
4. (d) Heatmap representation of the proteomic profile of THP-1 CAR-M treated with iTREM2 or control following stimulation with IFN-γ or IL-4/IL-10 for 24 h.
5. (e) Box plot representation of protein expression levels in THP-1 CAR-M treated with iTREM2 or control under IFN-γ or IL-4/IL-10 stimulation for 24 h.

# TREM2 inhibition enhances phagocytic activity of CAR-M

Given that TREM2 inhibition reprogrammed CAR-M toward a more pro-inflammatory phenotype and was associated with proteomic changes indicative of enhanced phagocytic capacity, including the down-regulation of inhibitory pathways and the upregulation of proteins involved in cytoskeletal remodeling, we next assessed whether this translated into enhanced functional activity. Phagocytosis was measured by flow cytometry using GFP-expressing macrophages and Cytotell Blue-labeled tumor cells, allowing quantification of double-positive ($GFP^+$/$Cytotell^+$) cells.

HER2 CAR-M and mock macrophages expressing either scramble shRNA or shTREM2 were co-cultured with HER2-positive AU565 cancer cells for 6 or 24 h, with or without IFN-γ stimulation. At 6 h, IFN-γ increased phagocytic activity; but no significant effect of TREM2 silencing was observed (**Fig. 7a-b**). In contrast, after 24 h, TREM2 knockdown significantly enhanced phagocytosis under basal conditions, with a further increase upon IFN-γ stimulation, resulting in an approximately two-fold increase (**Fig. 7a and 7b**). These findings support enhanced phagocytic potential after TREM2 inhibition. Immunofluorescence analysis further confirmed active engulfment of AU565 tumor cells by CAR-M following TREM2 inhibition (**Fig. 7c**).

To assess antigen specificity, similar experiments were performed using HER2-negative MDA-MB-231 cells. Phagocytic activity remained low across all conditions, with only minor differences between groups, confirming the HER2-dependent specificity of CAR-M-mediated phagocytosis (**Supp. Figure 5a**). A slight increase was observed at 24h for the shTREM2 CAR-M stimulated with IFN-γ, but the overall percentage of phagocytosis was substantially lower compared to HER2-positive targets (approximately 1.5% versus 9% double-positive cells).

We next evaluated pharmacological TREM2 inhibition. The inhibitor had minimal impact on AU565 viability (**Supp. Figure 6**). Treatment of HER2 CAR-M with the inhibitor resulted in earlier enhancement of phagocytosis, with increased activity observed at 6 h in the presence of IFN-γ, while effects at later time

points were less pronounced (**Fig. 7d-e**), suggesting that pharmacological inhibition may accelerate the onset of CAR-M activation. Immunofluorescence analysis further confirmed active engulfment of AU565 tumor cells by CAR-M following iTREM2 treatment (**Fig. 7f**). Similar to genetic inhibition, phagocytosis of HER2-negative cells remained low, with only a slight increase upon IFN-γ stimulation (**Supp. Figure 5b**).

As expected, mock macrophages displayed lower phagocytic activity than HER2 CAR-M across all conditions, confirming the contribution of CAR expression.

Finally, to validate these findings in a physiologically relevant model, we performed phagocytosis assays using patient-derived HER2-positive tumoroids. The HCI-032 tumoroid model was selected based on its high HER2 expression (**Supp. Figure 7**). TREM2 inhibition significantly enhanced CAR-M phagocytic activity after 48 h of co-culture, both under basal and IFN-γ-stimulated conditions (**Fig. 7g**), confirming the functional relevance of these observations.

Together, these results demonstrate that TREM2 acts as a negative regulator of CAR-M phagocytic activity and support its targeting to enhance macrophage-based immunotherapies.

**Figure 7 TREM2 inhibition enhances phagocytic activity of HER2 CAR macrophages.**

1. (a) Representative FACS plots showing phagocytosis of HER2-positive AU565 cancer cells by HER2 CAR-M and mock macrophages after 6 h and 24 h of co-culture at a 3:1 macrophage-to-cancer cell ratio. Phagocytosis was quantified as the percentage of double-positive Cytotell Blue$^+$/GFP$^+$ cells.
2. (b) Quantification of phagocytosis shown in (A) after 6 h and 24 h of co-culture under basal conditions or following IFN-γ stimulation (n = 3).
3. (c) Representative immunofluorescence images showing HER2 CAR-M engulfing AU565 tumor cells following TREM2 genetic inhibition. Macrophages are shown in green and tumor cells in blue.
4. (d) Representative FACS plots and (E, F) quantification of phagocytosis at 6 h and 24 h of co-culture, in the presence or absence of IFN-γ stimulation (n = 3) and iTREM2 inhibitor.

(e)Quantification of the phagocytosis from (A,B) after 6 and 24 hours of coculture (*n* = 3)

1. (f) Representative immunofluorescence images showing HER2 CAR-M engulfing AU565 tumor cells following iTREM2 treatment. Macrophages are shown in green and tumor cells in blue.
2. (g) Phagocytosis of patient-derived HER2-positive tumoroids by HER2 CAR-M under basal or IFN-γ–stimulated conditions, with or without TREM2 inhibition (n = 3).

# Discussion

In this study, we identify TREM2 as a key regulator of macrophage phenotype and function in breast cancer and CAR-M–based immunotherapy. Using transcriptomic data, in vitro functional assays, and proteomic analyses, we show that TREM2 is enriched in breast tumors and associated with immunosuppressive macrophage programs. Mechanistically, TREM2 promotes an anti-inflammatory phenotype and limits macrophage activation, whereas its inhibition induces a shift toward a pro-

inflammatory and metabolically active state. Importantly, TREM2 inhibition enhances the phagocytic activity of HER2-targeting CAR-M in a target-specific manner, including in patient-derived tumor models. Together, these findings identify TREM2 as a negative regulator of CAR-M anti-tumor activity.

TREM2 expression has been reported across multiple cancer types[16, 27–31]. In breast cancer, we show that TREM2 is increased in tumor tissues and associated with luminal and HER2-positive subtypes. Although TREM2 may have tumor-type-dependent roles[32–35], accumulating evidence indicates that it it is predominantly expressed in TAMs rather than tumor cells[36]. Our data support this view, as TREM2 correlated with myeloid and immunoregulatory signatures.

At the mechanistic level, our proteomic analyses show that TREM2 regulates key pathways involved in inflammation, immune regulation, and cellular metabolism. These results are consistent with previous observations that TREM2 is a critical regulator of immunometabolism, particularly in macrophages where it modulates glycolytic flux and lipid metabolism[37]. TREM2 inhibition also induced a shift toward interferon-driven and pro-inflammatory programs, while reducing IL-4/IL-10-associated signaling and tumor-associated macrophage features. Recent data also suggest a direct interaction between IL-4 and TREM2, further supporting its role in regulating macrophage polarization[38].

Notably, TREM2 appears to act as a dual regulator of macrophage phagocytosis by controlling both inhibitory checkpoints, such as SIRPA and CD300A, and pathways involved in cytoskeletal remodelling. This may explain the strong functional impact of TREM2 inhibition on macrophage anti-tumor activity and highlights its role as a central regulator of macrophage functional plasticity.

Functionally, these molecular changes translated into enhanced phagocytic activity of CAR-M. TREM2 inhibition increased phagocytosis in a target-specific manner and restored macrophage activity under immunosuppressive conditions, consistent with previous studies in glioblastoma[32, 39].

These findings have important implications for macrophage-based immunotherapies. TREM2 has been identified as a potential target in tumors resistant to immune checkpoint blockade and characterized by macrophage-rich microenvironments[40]. Our data suggest that TREM2 contributes to CAR-M dysfunction by promoting an anti-inflammatory state and limiting phagocytosis. Targeting TREM2 may therefore represent a strategy to enhance CAR-M efficacy by both relieving immunosuppression and boosting effector functions.

This study has some limitations. The use of the THP-1 cell line may not fully recapitulate primary macrophage biology, and in vivo studies will be required to validate the therapeutic potential of TREM2 targeting.

In conclusion, our study identifies TREM2 as a central regulator of macrophage phenotype and demonstrates that its inhibition enhances HER2 CAR-M anti-tumor activity, supporting its targeting to improve macrophage-based immunotherapies in breast cancer.

## Declarations

# Competing Interests

The authors have no relevant financial or non-financial interests to disclose.

# Ethics approval

The study was approved by the local research committee of the Oscar Lambret Cancer Center and a French Ethical Committee (IdRCB 2021-A00670-41). Written informed consent for the study was obtained from the patients.

# Funding

This work was supported by a PLBIO grant (N°2021-097) from the French National Cancer Institute, by the allocation dedicated to the team of the Ligue Contre le Cancer, by the Hauts-de-France Region, the University of Lille and the CPER Resistomics and Tec-Santé programmes.

# Author Contribution

Conceptualization and Methodology: MJ, LZC, MS and MD, Data curation and Writing – original draft: MJ, LZC and MD, Investigation : MJ, LZH, ARR, and MD, Writing – review and editing, Supervision and Funding acquisition: MS and MD, Formal Analysis, Validation and Visualization: MJ and LZC.

# Acknowledgement

We thank Nathalie Jouy and Emilie Floquet from the US 41 – UAR 2014 - PLBS for their help and advice with the flow cytometry experiments.We would like to thank the OrganOmics Core Facility of the University of Lille, which is accredited by the GIS IBiSA and is a member of the French Proteomics Infrastructure (ProFI) UAR 2048.

# Data Availability

Public transcriptomic datasets analyzed during the current study are available through TCGA/GTEx, GEPIA2 and cBioPortal. The data generated in this study, including MS raw files, DIA-NN files and annotated MS/MS datasets, have been deposited with the ProteomeXchange Consortium via the PRIDE partner repository.

# References


1. Gentles AJ, Newman AM, Liu CL, Bratman SV, Feng W, Kim D et al (2015) The prognostic landscape of genes and infiltrating immune cells across human cancers. Nat Med Nat Publishing Group 21:938–945. https://doi.org/10.1038/nm.3909
2. Mantovani A, Allavena P, Sica A, Balkwill F (2008) Cancer-related inflammation. Nat Nat Publishing Group 454:436–444. https://doi.org/10.1038/nature07205
3. Zhang J, Li S, Liu F, Yang K (2022) Role of CD68 in tumor immunity and prognosis prediction in pan-cancer. Sci Rep Nat Publishing Group 12:7844. https://doi.org/10.1038/s41598-022-11503-2
4. Jassaud M, Ziane-Chaouche L, Duhamel M, Salzet M (2026) Innate immune cells in chimeric antigen receptor therapy. Mol Ther J Am Soc Gene Ther 34:97–116. https://doi.org/10.1016/j.ymthe.2025.10.003
5. Klichinsky M, Ruella M, Shestova O, Lu XM, Best A, Zeeman M et al (2020) Human chimeric antigen receptor macrophages for cancer immunotherapy. Nat Biotechnol Nat Publishing Group 38:947–953. https://doi.org/10.1038/s41587-020-0462-y
6. Ziane-Chaouche L, Raffo-Romero A, Hajjaji N, Kobeissy F, Pinheiro D, Aboulouard S et al (2024) Inhibition of furin in CAR macrophages directs them toward a proinflammatory phenotype and enhances their antitumor activities. Cell Death Dis Nat Publishing Group 15:879. https://doi.org/10.1038/s41419-024-07267-4
7. Lei A, Yu H, Lu S, Lu H, Ding X, Tan T et al (2024) A second-generation M1-polarized CAR macrophage with antitumor efficacy. Nat Immunol Nat Publishing Group 25:102–116. https://doi.org/10.1038/s41590-023-01687-8
8. Duan Z, Li Z, Wang Z, Chen C, Luo Y (2023) Chimeric antigen receptor macrophages activated through TLR4 or IFN-γ receptors suppress breast cancer growth by targeting VEGFR2. Cancer Immunol Immunother CII 72:3243–3257. https://doi.org/10.1007/s00262-023-03490-8
9. Feng M, Jiang W, Kim BYS, Zhang CC, Fu Y-X, Weissman IL (2019) Phagocytosis checkpoints as new targets for cancer immunotherapy. Nat Rev Cancer Nat Publishing Group 19:568–586. https://doi.org/10.1038/s41568-019-0183-z
10. Liu Y, Wang Y, Yang Y, Weng L, Wu Q, Zhang J et al (2023) Emerging phagocytosis checkpoints in cancer immunotherapy. Signal Transduct Target Ther Nat Publishing Group 8:104. https://doi.org/10.1038/s41392-023-01365-z
11. Ulland TK, Song WM, Huang SC-C, Ulrich JD, Sergushichev A, Beatty WL et al (2017) TREM2 Maintains Microglial Metabolic Fitness in Alzheimer's Disease. Cell 170:649–663e13. https://doi.org/10.1016/j.cell.2017.07.023
12. Wang S, Mustafa M, Yuede CM, Salazar SV, Kong P, Long H et al (2020) Anti-human TREM2 induces microglia proliferation and reduces pathology in an Alzheimer's disease model. J Exp Med 217:e20200785. https://doi.org/10.1084/jem.20200785

13. Nakamura K, Smyth MJ (2020) TREM2 marks tumor-associated macrophages. Signal Transduct Target Ther. Nat Publishing Group 5:233. https://doi.org/10.1038/s41392-020-00356-8
14. Katzenelenbogen Y, Sheban F, Yalin A, Yofe I, Svetlichnyy D, Jaitin DA et al (2020) Coupled scRNA-Seq and Intracellular Protein Activity Reveal an Immunosuppressive Role of TREM2 in Cancer. Cell 182:872–885e19. https://doi.org/10.1016/j.cell.2020.06.032
15. Zhang H, Liu Z, Wen H, Guo Y, Xu F, Zhu Q et al (2022) Immunosuppressive TREM2(+) macrophages are associated with undesirable prognosis and responses to anti-PD-1 immunotherapy in non-small cell lung cancer. Cancer Immunol Immunother CII 71:2511–2522. https://doi.org/10.1007/s00262-022-03173-w
16. Sun R, Han R, McCornack C, Khan S, Tabor GT, Chen Y et al (2023) TREM2 inhibition triggers antitumor cell activity of myeloid cells in glioblastoma. Sci Adv Am Association Advancement Sci 9:eade3559. https://doi.org/10.1126/sciadv.ade3559
17. Guillen KP, Fujita M, Butterfield AJ, Scherer SD, Bailey MH, Chu Z et al (2022) A human breast cancer-derived xenograft and organoid platform for drug discovery and precision oncology. Nat Cancer Nat Publishing Group 3:232–250. https://doi.org/10.1038/s43018-022-00337-6
18. Raffo-Romero A, Ziane-Chaouche L, Salomé-Desnoulez S, Hajjaji N, Fournier I, Salzet M et al (2024) A co-culture system of macrophages with breast cancer tumoroids to study cell interactions and therapeutic responses. Cell Rep Methods [Internet]. Elsevier; [cité 29 avr 2026];4. https://doi.org/10.1016/j.crmeth.2024.100792
19. Demichev V, Szyrwiel L, Yu F, Teo GC, Rosenberger G, Niewienda A et al (2022) dia-PASEF data analysis using FragPipe and DIA-NN for deep proteomics of low sample amounts. Nat Commun 13:3944. https://doi.org/10.1038/s41467-022-31492-0
20. Demichev V, Messner CB, Vernardis SI, Lilley KS, Ralser M (2020) DIA-NN: Neural networks and interference correction enable deep proteome coverage in high throughput. Nat Methods 17:41–44. https://doi.org/10.1038/s41592-019-0638-x
21. Zirem Y, Ledoux L, Fournier I, Salzet M (2026) Profiler: an open web platform for multi-omics analysis. Bioinformatics 42:btaf644. https://doi.org/10.1093/bioinformatics/btaf644
22. Yang T, Zhang S, Yuan H, Wang Y, Cai L, Chen H et al (2023) Platinum-Based TREM2 Inhibitor Suppresses Tumors by Remodeling the Immunosuppressive Microenvironment. Angew Chem 135:e202213337. https://doi.org/10.1002/ange.202213337
23. Bego MG, Mercier J, Cohen EA (2012) Virus-activated interferon regulatory factor 7 upregulates expression of the interferon-regulated BST2 gene independently of interferon signaling. J Virol 86:3513–3527. https://doi.org/10.1128/JVI.06971-11
24. Wu N, Nguyen X-N, Wang L, Appourchaux R, Zhang C, Panthu B et al (2019) The interferon stimulated gene 20 protein (ISG20) is an innate defense antiviral factor that discriminates self versus non-self translation. PLoS Pathog 15:e1008093. https://doi.org/10.1371/journal.ppat.1008093

25. Kim HS, Kim DC, Kim H-M, Kwon H-J, Kwon SJ, Kang S-J et al (2015) STAT1 deficiency redirects IFN signalling toward suppression of TLR response through a feedback activation of STAT3. Sci Rep 5:13414. https://doi.org/10.1038/srep13414
26. Winkels H, Meiler S, Smeets E, Lievens D, Engel D, Spitz C et al (2017) CD70 limits atherosclerosis and promotes macrophage function. Thromb Haemost 117:164–175. https://doi.org/10.1160/TH16-04-0318
27. Wu SZ, Al-Eryani G, Roden D, Junankar S, Harvey K, Andersson A et al (2021) A single-cell and spatially resolved atlas of human breast cancers. Nat Genet 53:1334–1347. https://doi.org/10.1038/s41588-021-00911-1
28. Katzenelenbogen Y, Sheban F, Yalin A, Yofe I, Svetlichnyy D, Jaitin DA et al (2020) Coupled scRNA-Seq and Intracellular Protein Activity Reveal an Immunosuppressive Role of TREM2 in Cancer. Cell Elsevier 182:872–885e19. https://doi.org/10.1016/j.cell.2020.06.032
29. Zhang Z, Yu K, Cao Y, Xie P, Wang L, Shen Z et al (2025) TREM2 facilitates gastric cancer progression and immune evasion via inhibiting TRIM21-mediated STAT1 degradation in tumor-associated macrophages. Cell Death Dis Nat Publishing Group 16:845. https://doi.org/10.1038/s41419-025-08198-4
30. Zhou L, Wang M, Guo H, Hou J, Zhang Y, Li M et al (2022) Integrated Analysis Highlights the Immunosuppressive Role of TREM2 + Macrophages in Hepatocellular Carcinoma. Front Immunol [Internet] Front. [cité 17 avr 2026];13 https://doi.org/10.3389/fimmu.2022.848367
31. Cheng X, Wang X, Nie K, Cheng L, Zhang Z, Hu Y et al (2021) Systematic Pan-Cancer Analysis Identifies TREM2 as an Immunological and Prognostic Biomarker. Front Immunol 12:646523. https://doi.org/10.3389/fimmu.2021.646523
32. Kim S-M, Kim E-M, Ji K-Y, Lee H-Y, Yee S-M, Woo S-M et al (2019) TREM2 Acts as a Tumor Suppressor in Colorectal Carcinoma through Wnt1/β-catenin and Erk Signaling. Cancers Multidisciplinary Digit Publishing Inst 11:1315. https://doi.org/10.3390/cancers11091315
33. Wang X-Q, Tao B-B, Li B, Wang X-H, Zhang W-C, Wan L et al (2015) Overexpression of TREM2 enhances glioma cell proliferation and invasion: a therapeutic target in human glioma. Oncotarget Impact Journals 7:2354–2366. https://doi.org/10.18632/oncotarget.6221
34. Gao H-T, Yang Z, Sun H, Zhang Y, Wang Z, Liu W-Y et al (2023) TREM2 as an independent predictor of poor prognosis promotes the migration via the PI3K/AKT axis in prostate cancer. Am J Transl Res 15:779–798
35. Wang J, Li Z (2022) TREM2 Is a Prognostic Biomarker and Correlated with an Immunosuppressive Microenvironment in Thyroid Cancer. Dis Markers 2022:1807386. https://doi.org/10.1155/2022/1807386
36. Nakamura K, Smyth MJ (2020) TREM2 marks tumor-associated macrophages. Signal Transduct Target Ther. Nat Publishing Group 5:233. https://doi.org/10.1038/s41392-020-00356-8
37. Che Y, Yu Z, Ji S, Yang D (2026) Decoding TREM2 Signaling Pathways. Neurol Neuroimmunol Neuroinflammation 13:e200527. https://doi.org/10.1212/NXI.0000000000200527

38. Zhu X, Zhang C, Jiang W, Zeng Z, Zhang K, Du M et al (2024) Trem2 acts as a non-classical receptor of interleukin-4 to promote diabetic wound healing. Clin Transl Med 14:e70026. https://doi.org/10.1002/ctm2.70026
39. Zheng J, Wang L, Zhao S, Zhang W, Chang Y, Bosco DB et al (2024) TREM2 mediates MHCII-associated CD4 + T-cell response against gliomas. Neuro-Oncol 26:811–825. https://doi.org/10.1093/neuonc/noad214
40. Binnewies M, Pollack JL, Rudolph J, Dash S, Abushawish M, Lee T et al (2021) Targeting TREM2 on tumor-associated macrophages enhances immunotherapy. Cell Rep [Internet] Elsevier. [cité 17 avr 2026];37 https://doi.org/10.1016/j.celrep.2021.109844

# Figures

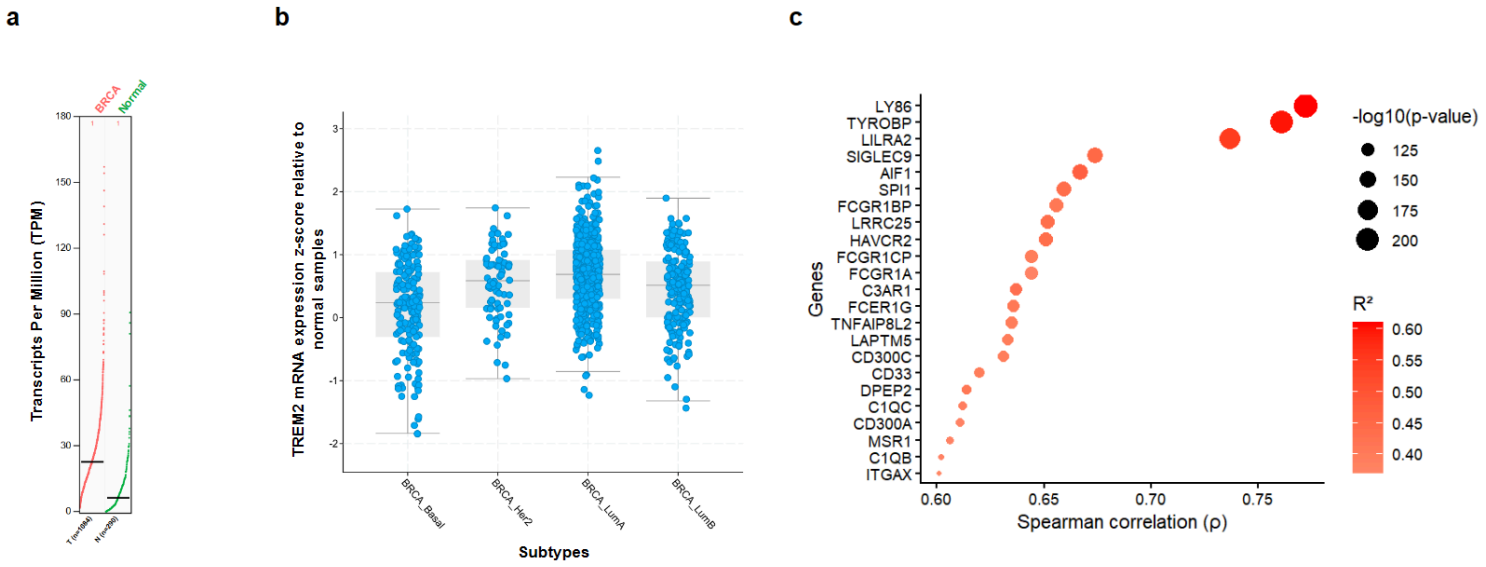


**Figure 1**

**TREM2 is upregulated in breast cancer and associated with a myeloid immune transcriptional program.**

(a) TREM2 expression in breast cancer (BRCA) compared to normal breast tissue using TCGA RNA-seq data, showing increased expression in tumor samples.

(b) TREM2 mRNA expression across breast cancer molecular subtypes (Basal-like, HER2-enriched, Luminal A, and Luminal B) using TCGA data, represented as z-scores relative to normal tissues.

(c) Spearman correlation analysis of TREM2 expression with immune-related genes in breast cancer samples. Dot size represents statistical significance (-log10 p-value) and color intensity represents correlation strength ($R^2$).

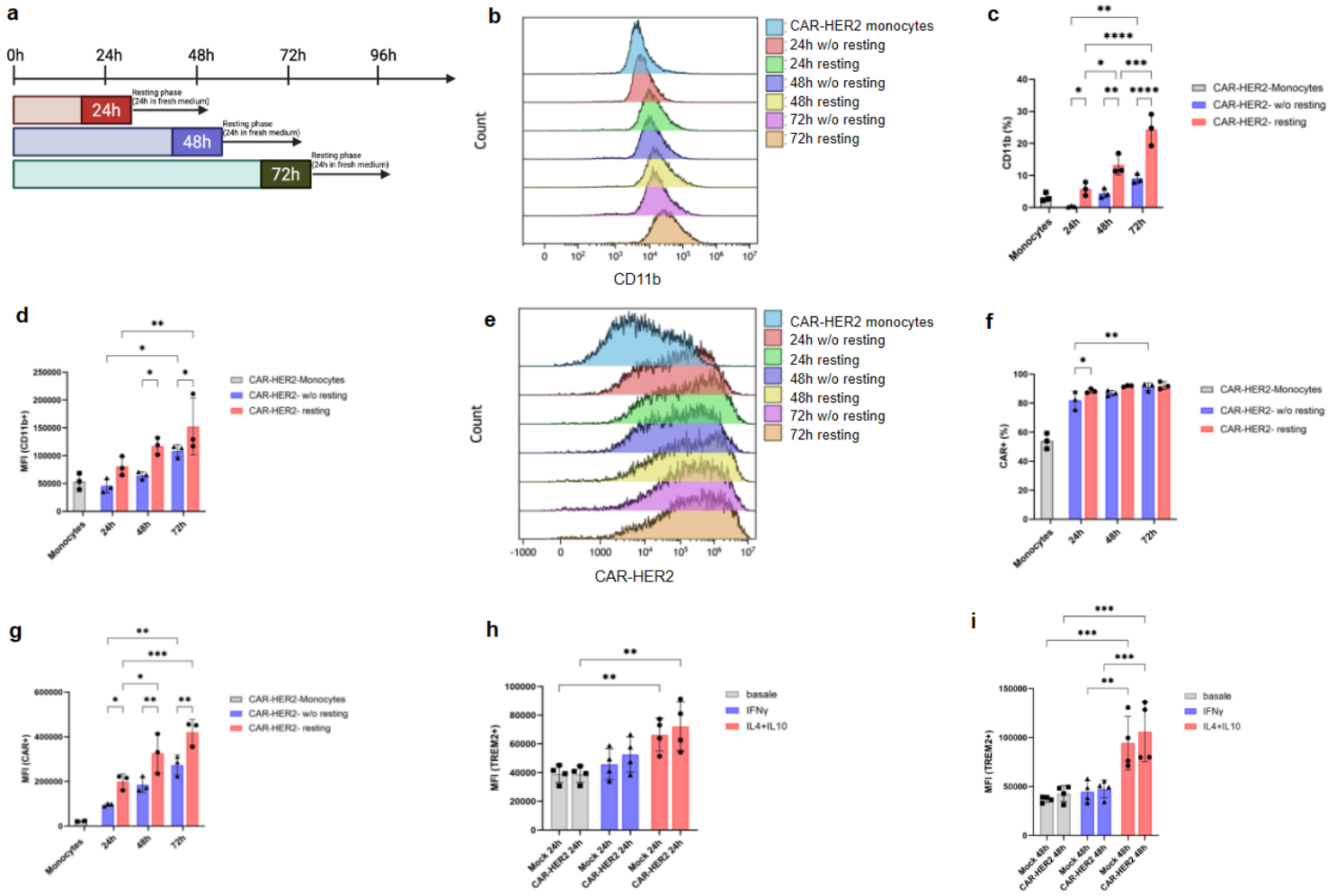


## Figure 2

**Optimization of HER2 CAR macrophage differentiation and regulation of TREM2 expression by macrophage polarization**

(a) Experimental design illustrating the differentiation and resting kinetics of CAR-HER2 kinetics of CAR-HER2 monocytes at 24 h, 48 h, and 72 h.

(b) Representative flow cytometry histograms showing CD11b expression in CAR-HER2 monocytes at different time points, with or without a resting phase.

(c-d) Quantification of CD11b expression, shown as the percentage of $CD11b^+$ cells and mean fluorescence intensity (MFI) (n=3).

(e) Representative histograms of CAR expression in CAR-HER2 cells with or without a resting phase.

(f-g) Quantification of CAR expression, shown as the percentage of CAR-positive cells and MFI (n=3).

(h-i) TREM2 expression (MFI) at 24 h and 48 h following stimulation with IFNγ or IL-4/IL-10 (n=3).

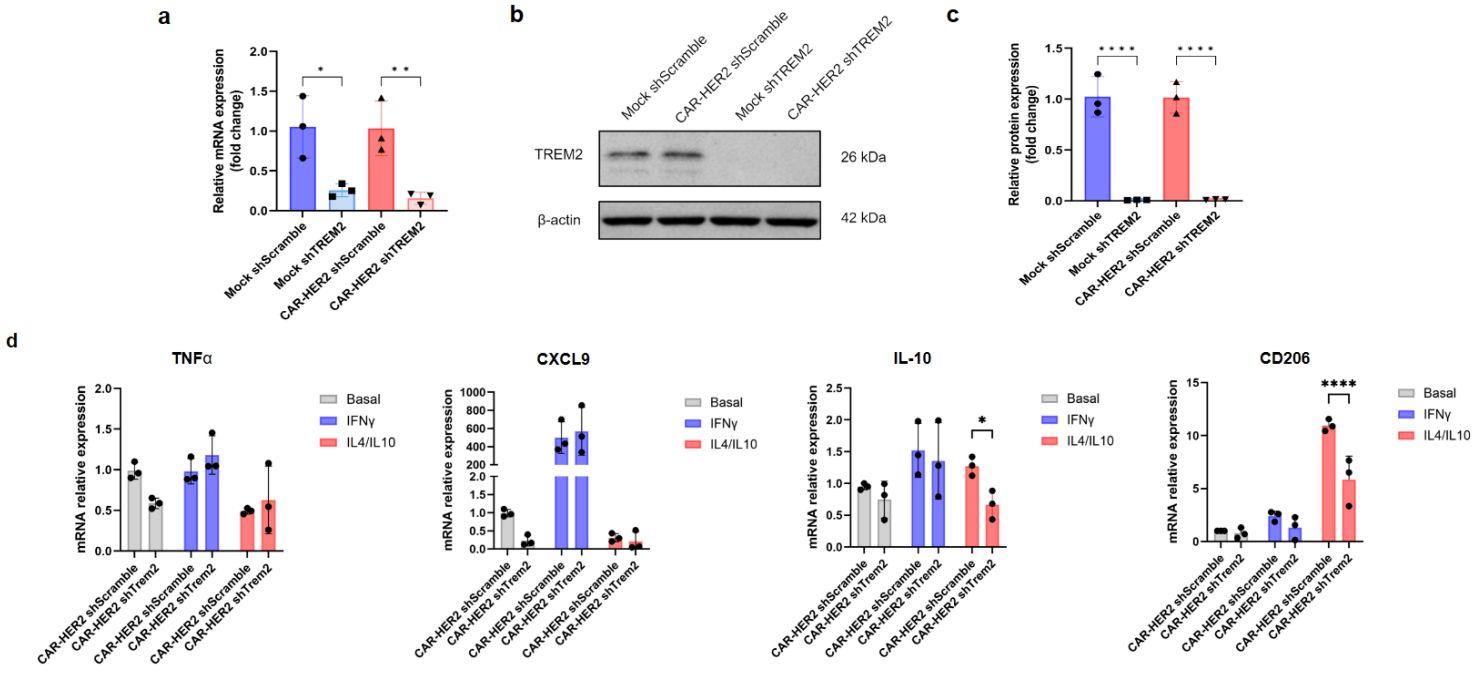


## Figure 3

**Genetic inhibition of TREM2 modulates macrophage polarization in HER2 CAR macrophages**

(a) Relative TREM2 mRNA expression in mock and CAR-HER2 macrophages transduced with scramble or shTREM2 constructs (n=3).

(b) Representative Western blot analysis of TREM2 protein expression in mock and CAR-HER2 macrophages, with β-actin as a loading control (n=3).

(c) Quantification of TREM2 protein expression relative to β-actin (n=3).

(d) Relative mRNA expression of polarization-associated genes in CAR-HER2 macrophages (scramble vs shTREM2) under basal conditions or following stimulation with IFNγ or IL-4/IL-10 (n=3).

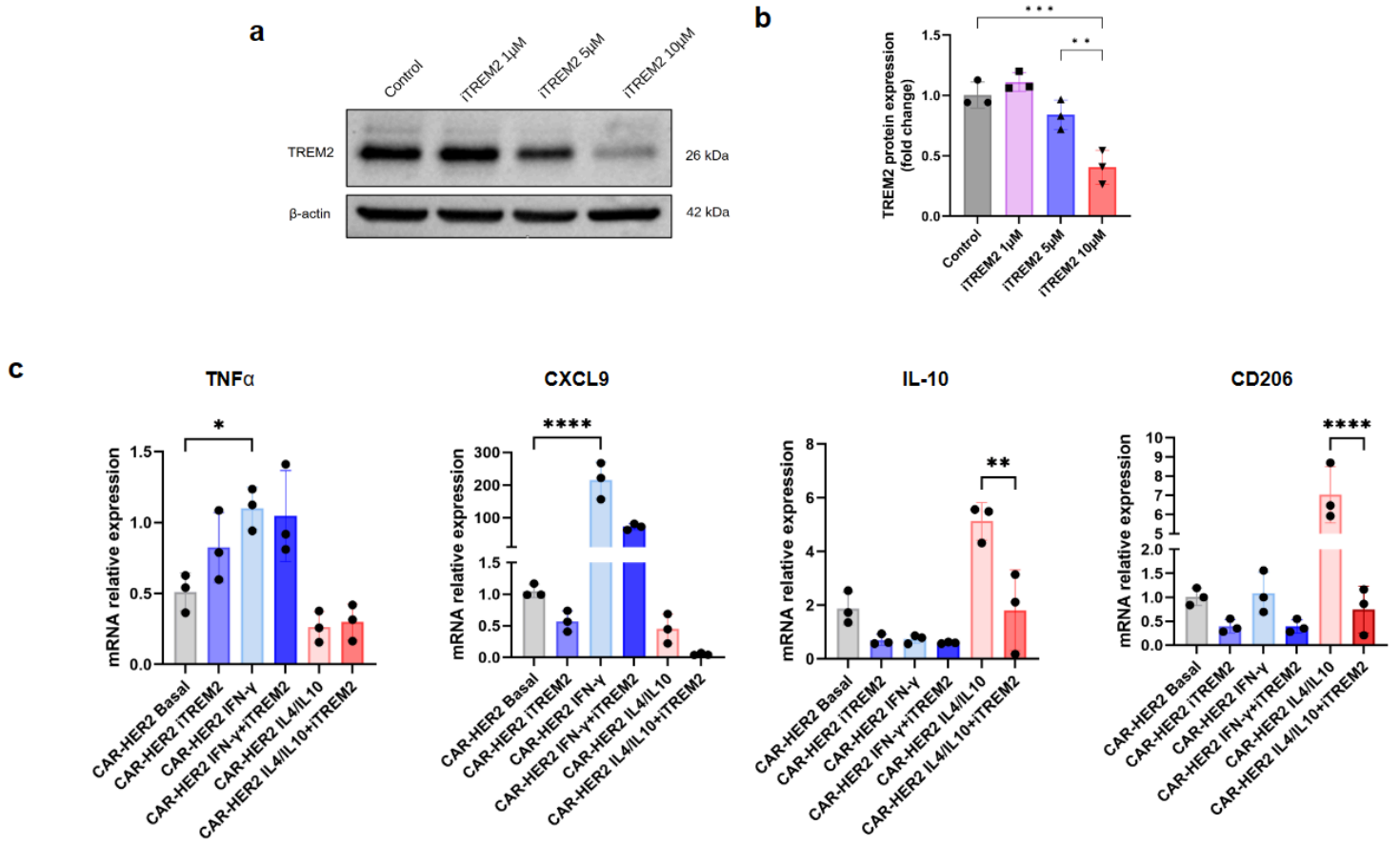


## Figure 4

**Pharmacological inhibition of TREM2 modulates macrophage polarization in HER2 CAR macrophages.**

(a) Western blot analysis of TREM2 protein expression following treatment with increasing concentrations of the TREM2 inhibitor (iTREM2), with β-actin as a loading control (n = 3).

(b) Quantification of TREM2 protein expression following iTREM2 treatment. TREM2 levels were normalized to β-actin and expressed as fold change relative to untreated control macrophages (n = 3).

(c) Relative mRNA expression of polarization-associated genes (TNF-α, CXCL9, IL-10 and CD206) in CAR-HER2 macrophages under basal conditions or following stimulation with IFN-γ or IL-4/IL-10, in the presence or absence of the TREM2 inhibitor (iTREM2) (n = 3).

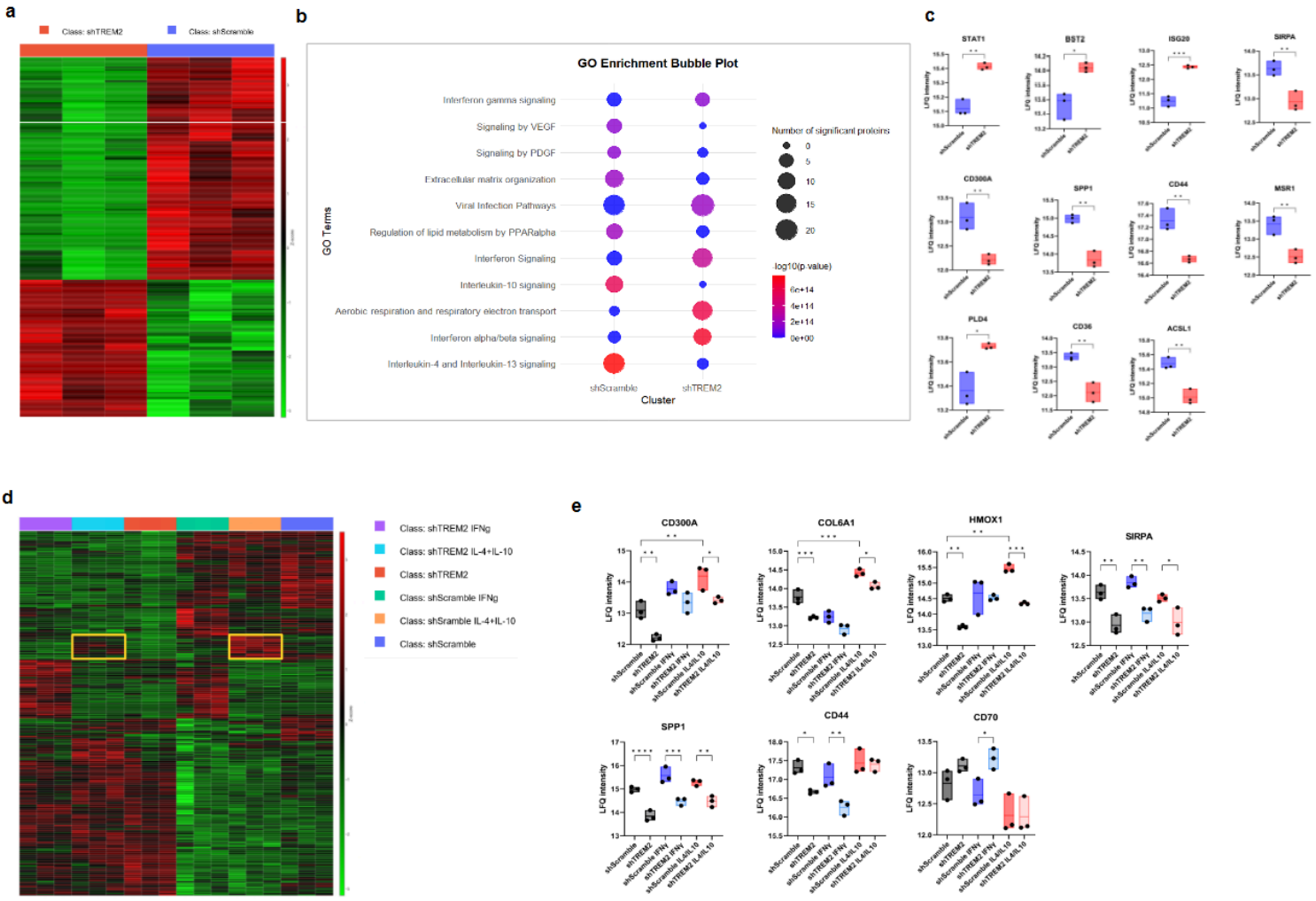


## Figure 5

**Genetic inhibition of TREM2 reshapes the proteomic landscape of HER2 CAR macrophages.**

(a) Heatmap representation of the proteomic profile of THP-1 CAR-M following transduction with shTREM2 or scramble shRNA.

(b) Bubble plot showing enriched Reactome pathways in THP-1 CAR-M shTREM2 compared to scramble controls.

(c) Box plot representation of protein expression levels in THP-1 CAR-M shTREM2 versus scramble controls.

(d) Heatmap representation of the proteomic profile of THP-1 CAR-M (shTREM2 vs scramble) following stimulation with IFN-γ or IL-4/IL-10 for 24 h.

(e) Box plot representation of protein expression levels in THP1 CAR-M (shTREM2 vs scramble) under IFN-γ or IL-4/IL-10 stimulation for 24 h.

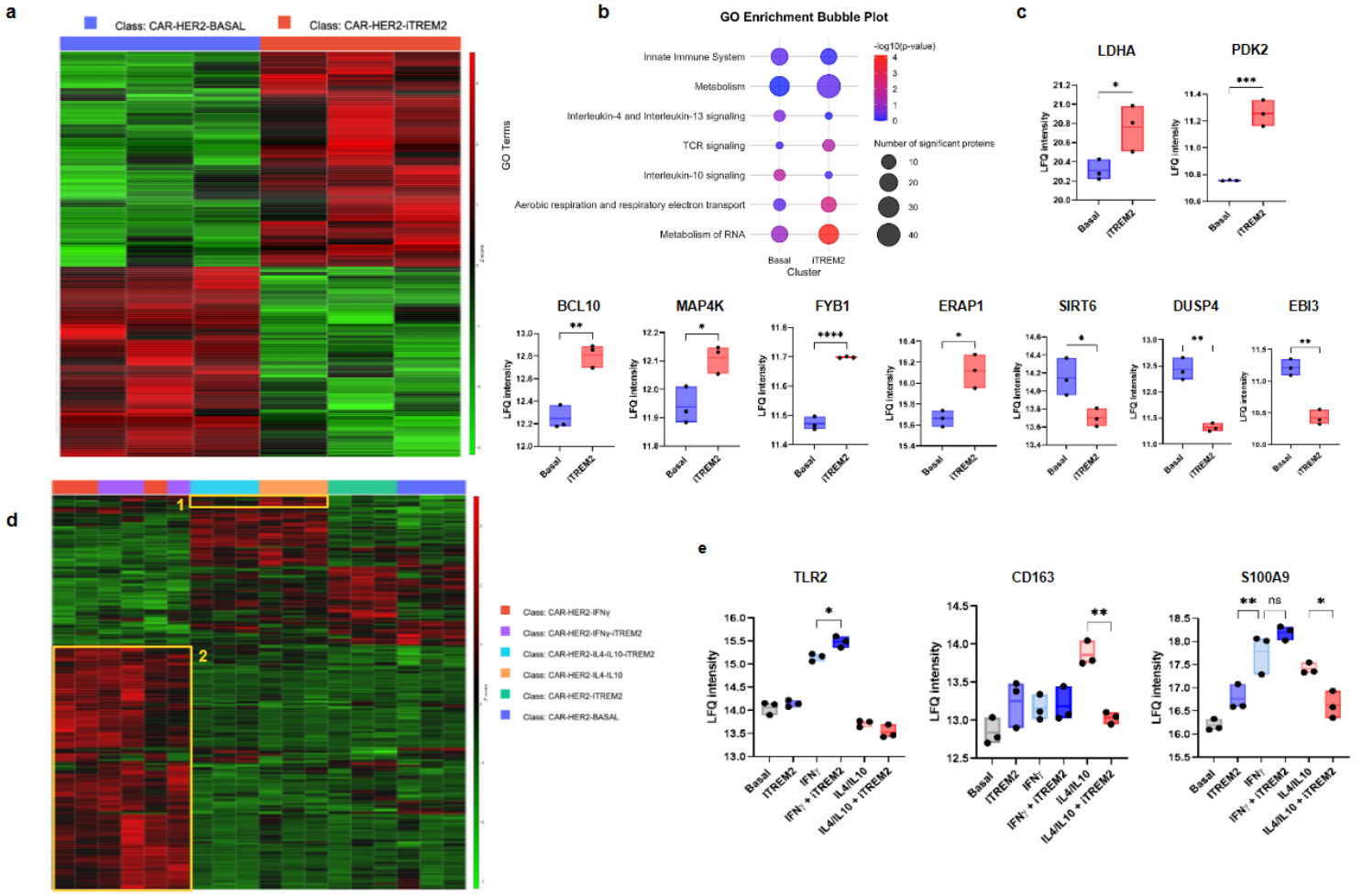


## Figure 6

**Pharmacological inhibition of TREM2 reshapes the proteomic landscape of HER2 CAR macrophages.**

(a) Heatmap representation of the proteomic profile of THP-1 CAR-M following treatment with the iTREM2 inhibitor or control.

(b) Bubble plot showing enriched Reactome pathways in THP-1 CAR-M treated with iTREM2 compared to control.

(c) Box plot representation of protein expression levels in THP-1 CAR-M treated with iTREM2 versus control.

(d) Heatmap representation of the proteomic profile of THP-1 CAR-M treated with iTREM2 or control following stimulation with IFN-γ or IL-4/IL-10 for 24 h.

(e) Box plot representation of protein expression levels in THP-1 CAR-M treated with iTREM2 or control under IFN-γ or IL-4/IL-10 stimulation for 24 h.

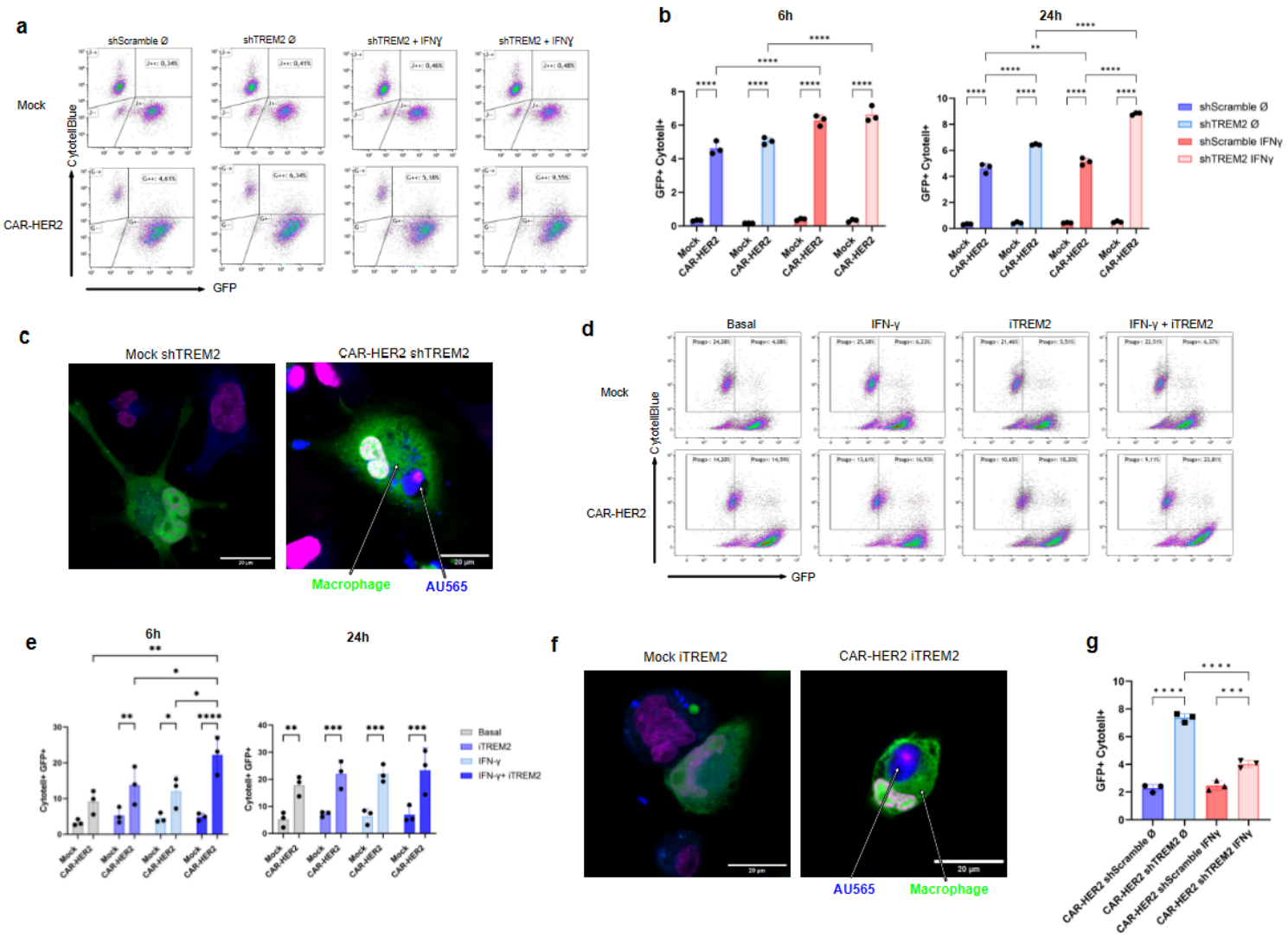


## Figure 7

**TREM2 inhibition enhances phagocytic activity of HER2 CAR macrophages.**

(a) Representative FACS plots showing phagocytosis of HER2-positive AU565 cancer cells by HER2 CAR-M and mock macrophages after 6 h and 24 h of co-culture at a 3:1 macrophage-to-cancer cell ratio. Phagocytosis was quantified as the percentage of double-positive Cytotell Blue⁺/GFP⁺ cells.

(b) Quantification of phagocytosis shown in (A) after 6 h and 24 h of co-culture under basal conditions or following IFN-γ stimulation (n = 3).

(c) Representative immunofluorescence images showing HER2 CAR-M engulfing AU565 tumor cells following TREM2 genetic inhibition. Macrophages are shown in green and tumor cells in blue.

(d) Representative FACS plots and (E, F) quantification of phagocytosis at 6 h and 24 h of co-culture, in the presence or absence of IFN-γ stimulation (n = 3) and iTREM2 inhibitor.

(e)Quantification of the phagocytosis from (A,B) after 6 and 24 hours of coculture (*n* = 3)

(f) Representative immunofluorescence images showing HER2 CAR-M engulfing AU565 tumor cells following iTREM2 treatment. Macrophages are shown in green and tumor cells in blue.

(g) Phagocytosis of patient-derived HER2-positive tumoroids by HER2 CAR-M under basal or IFN-γ–stimulated conditions, with or without TREM2 inhibition (n = 3).

## Supplementary Files

This is a list of supplementary files associated with this preprint. Click to download.

- Supplementarytables.pdf
- Supplementaryfigures.pdf